

OPALISATION OF FOSSIL BONE AND WOOD: CLUES TO THE FORMATION OF PRECIOUS OPAL

Benjamath Pewkliang^{1,2}, Allan Pring² & Joël Brugger^{1,2}

¹CRC LEME, School of Earth and Environmental Science, University of Adelaide, SA, 5005

²Department of Mineralogy, South Australian Museum, North Terrace, Adelaide 5000, South Australia

INTRODUCTION

The process of mineralisation of bone and shell for preservation in the fossil record is dependant on the chemical and physical conditions during diagenesis, particularly the composition of the mineralizing fluid. Fundamentally these processes can be considered as mineral replacement reactions, where the biomineral is replaced by another mineral such as quartz, opal or calcite. The replacement reaction can also be associated with recrystallisation of the biomineral, particularly bioapatite (carbonatehydroxylapatite), during which trace amounts of heavy metals may be incorporated into the apatite structure (Hubert *et al.* 1996). For the very fine scale microstructure of the fossil to be preserved, the dissolution of the biomineral must be tightly coupled to the precipitation reaction, so that no free space occurs at the reaction front (Putnis 2002). Such replacement reactions therefore proceed as the fluid fronts move through the fossil. If the dissolution and precipitation reactions are not tightly coupled and there is a gap between the dissolution front and the precipitation front fine details of the microstructure will not be preserved.

The processes leading to the formation of precious opal and the opalisation of fossils in the Australian opal deposits are poorly understood. There is considerable debate about the age of the opal. Barker (1980) and others concluded that opalisation occurred in the Late Cretaceous and is more or less contemporaneous with the stratigraphy. Horton (2002), however, proposes that opal deposition occurred after gentle warping at 24 Ma and thus much later than the deposition of the Cretaceous sediments in which it is found. Recent ¹⁴C dating of black opal from Lightning Ridge reveals Quaternary ages for the organic matter in these opals (Dowell & Mavrogenes 2004). Also there are debates about the source of the silica, the composition of the opalising fluids and the mechanism of precious opal formation in the Australian deposits (see Barnes *et al.* 1992 for overview). In much of the world, precious opal is formed from volcanic fluids. Indeed volcanic opal is a very common phase resulting from hydrothermal alteration of felsic volcanics by acid sulfate fluids and from the boiling and/or mixing of neutral chloride geothermal brines in epithermal settings (Corbett & Leach 1998). However in Australia, which produces 95% of the world's precious opal, the opal is thought to be of sedimentary origin. On the Australian fields, opal occurs in veins and nodules within clay layers in shales and sandstones. Precious and potch opal are also found replacing, shells, wood and less frequently, the bones and teeth of marine reptiles (Barnes *et al.* 1992). The skeletons of Cretaceous plesiosaurs and ichthyosaurs that have been partially or completely opalized have been found at Andamooka, Coober Pedy and White Cliffs (Kear 2003).

We report here the preliminary results of a detailed investigation of the chemistry, structure and microstructure of opalised marine reptile bones from Andamooka and Coober Pedy and opalised wood from White Cliffs. This material is compared to samples of opalised wood from Nevada, where opalisation is known to be associated with volcanism and also with samples of ichthyosaur bone from near Coober Pedy that have not been opalised.

LOCATION AND DEPOSITIONAL FRAMEWORK

The opalised fossils at Coober Pedy and Andamooka are found within the opal-bearing layers of the Cretaceous Bulldog Shale (Barremian-Early Albian), whereas at White Cliffs they are found within the Doncaster Member of the Wallumbilla Formation (Late Barremian-Aptian). Both precious and potch opal are found in the weathered Bulldog Shale as subhorizontal to subvertical veins infilling cracks and joints. The stratigraphy and geology of Andamooka and Coober Pedy are similar and opal is commonly found as horizontal beds known as the opal level (Jones & Segnit 1966). Opal veins cutting across the opal level and pore fillings in a band of clay and conglomerate within the Bulldog Shale are also common.

Coober Pedy and Andamooka lie within the Eromanga Basin, which is a part of the Great Artesian Basin, and during the Early and Middle Cretaceous (Aptian-Albian), was covered by a shallow sea. Over this period the area of the Great Artesian Basin received remarkably uniform, fine grained, terrigenous sediments and the northern and eastern margins of the Eromanga Basin accumulated mud, silts and very fine sands of some 2,000 feet in thickness which have lain virtually undisturbed since the Cretaceous (Day 1969).

SAMPLES AND METHODS

Details of the samples examined in this study are summarized in Table 1. Polished thin-sections or polished mounts were prepared for all of the samples. The mineralogy and the crystallinity of the samples were determined using a HUBER Imaging Plate Guinier X-ray diffraction camera (670 model) with Co $K\alpha_1$ radiation. Bulk major and trace element analyses were undertaken using a Philips XRF analyzer on a fused disc made from the melting of the powdered sample and a pressed powder disc. A CAMECA SX51 electron microprobe using a WDS analysis system was used for microprobe analyses and elemental mapping. The analyses were carried out using accelerating potential of 15 kV and a sample current of 15 nA, with a beam diameter of 2-3 μm . Backscattered electron and secondary electron imaging of the surfaces of polished blocks and thin sections were obtained using a Philips XL30 Field Emission Gun Scanning Electron Microscope (SEM). In order to image the underlying microstructure at the resolution of the individual silica spheres of opal, selected polished blocks were etched in a solution of 10 M hydrofluoric acid for 30 seconds. These samples were then washed and dried before sputter coating with a thin conducting layer of Au. Images of the samples were obtained at either 10 kV or 15 kV. The EDS spectra were also recorded during examination of the opal samples on the XL30 SEM.

Table 1: Summary of the samples examined in the study.

Sample	Description	"State"	Location/Formation	Petrologic thin section	XRD
A	wood opal	opalised	Nevada, USA	Dominant-Am Traces-Trd, carbonate	Trd, O
B	fibrous opal	opalised	Columbus mining district, Nevada, USA	Dominant-Am Traces: Trd (very fine)	Trd, O
C	opal replacing wood	opalised	Columbia district, Nevada, USA	Dominant-Am Traces: Qtz (Trd and/or Crs)	Trd, Qtz, O, Crs
D	fossilised wood	fossilised	Cooper Pedy, SA/Bulldog Shale	Dominant-Am, Qtz Traces-tridymite	Trd, Cal, Py
E	opalised wood	opalised	White Cliffs	Dominant-opaline Am Traces-chalcedony	O, Py, Crs
F	opalised shell	opalised	White Cliffs?		Qtz, Gp, Cal
G	Ichthyosaur limb of <i>Platypterygius longmani</i>	fossilised	Moon Plain, 40 km N of Cooper Pedy, SA		Cal, Ap
H	ichthyosaur	fossilised	London/heme Raqs		Cal, Ap, Qtz
I	Plesiosaur limb	opalised	Andamooka/Bulldog Shale		Qtz, Ap, O, Py
J	Plesiosauroidea indet Miscellaneous fragment	opalised	Andamooka opal field, SA/Bulldog Shale		Qtz, Ap, O
K	Plesiosauroidea indet neural arch fragment	opalised	Andamooka opal field, SA/Bulldog Shale		Qtz, Ap, O
L	Plesiosauroidea indet rib/girdle fragments	opalised	Andamooka opal field, SA/Bulldog Shale		Qtz, Ap, O
M	Plesiosauroidea indet limb/rib fragments	opalised	Andamooka opal field, SA/Bulldog Shale		Qtz, Ap, O
N	Dolphin rib bone	modern	Fowlers Bay, Australia		Ap

Tridymite (Trd); Quartz (Qtz), Calcite (Cal), Pyrite (Py), carbonate hydroxylapatite (Ap), Opal (O), Gypsum (Gp), Cristobalite (Crs), Amorphous SiO_2 (Am)

RESULTS

Chemical composition

The results of the major and trace element analyses for the samples are summarized in Table 2. The elemental analyses show that the opalised bone and wood are essentially pure SiO_2 with minor amounts of Al_2O_3 (probably present as clay inclusions) and the opalised bone samples contain no remnant bioapatite. This is consistent with the bone structure having been completely opalised. The trace element analysis, when normalized to the Post Archean average shale (PAAS), shows that the opal is depleted in all trace elements with the exception of Zr. Zr probably occurs in detrital minerals (e.g., zircon), as is shown by the coarse correlation between Al_2O_3 and ZrO contents.

Table 2: The results of the major and trace element analyses for some of the samples.

	C	D	E	F	G	H	I	J	K	N
SiO ₂ %	84.58	4.0	91.8	87.7	2.27	0.93	91.87	88.59	92.69	0.15
Al ₂ O ₃ %	0.26	0.1	2.1	2.9	0.76	0.21	2.12	4.41	2.02	0.04
Fe ₂ O ₃ (tot) %	0.02	1.6	0.1	0.5	0.93	0.77	0.33	0.58	0.22	0.07
MnO %	0.01	0.5	0.0	0.0	0.59	0.03	0.01	0.01	0.01	0.01
MgO %	0.01	2.0	0.1	0.1	7.42	1.08	0.04	0.26	0.09	1.10
CaO %	1.19	45.6	0.2	1.7	40.29	46.88	0.10	0.15	0.06	35.41
Na ₂ O %	0.26	0.4	0.3	0.4	0.61	0.91	0.31	0.36	0.28	0.77
K ₂ O %	0.02	0.0	0.1	0.4	0.08	0.02	0.09	0.19	0.07	0.01
TiO ₂ %	0.00	0.1	0.1	0.6	0.07	0.04	0.12	0.53	0.16	0.02
P ₂ O ₅ %	0.01	1.0	0.0	0.0	12.30	27.30	0.01	0.01	0.00	26.00
SO ₃ %	0.05	0.2	0.0	1.2	5.27	1.23	0.01	0.00	0.01	1.43
LOI %	13.78	40.5	4.1	4.7	26.99	14.48	4.16	4.23	3.63	31.88
Total %	100.18	95.8	98.9	100.1	97.57	93.97	99.16	99.30	99.23	96.88
Zr (ppm)	8.2	7.8	199.0	206.0	16.4	26.2	232.4	267.2	211.7	5.5
Nb (ppm)	0.1	0.9	1.7	6.4	-0.1	4.4	2.6	5.7	1.8	0
Y (ppm)	24.9	2.0	1.5	5.2	7	863.4	2.4	3.8	2.1	0
Sr (ppm)	100.2	583.5	47.2	134.4	720.7	3127.6	16.5	25.1	14.7	290.2
Rb (ppm)	1.1	0.6	13.2	14.0	4.9	3.6	10.9	15.3	8.8	0.5
U (ppm)	48.1	2.4	0.2	1.0	2.0	56.1	1.7	2.4	0.5	-0.1
Th (ppm)	2.4	2.4	1.3	3.6	0.7	5.6	1.0	1.3	1.9	2.7
Pb (ppm)	0.4	1.3	2.2	6.4	0.4	4.6	2.6	1.6	2.6	1.6
Ga (ppm)	2.4	0.0	3.5	5.6	0.3	-0.3	3.2	6.6	4.1	1.1
Cu (ppm)	11.0	0.0	2.0	5.0	8.0	0.0	4.0	8.0	6.0	15.0
Zn (ppm)	3.0	11.0	2.0	3.0	67.0	104.0	15.0	114.0	16.0	678.0
Ni (ppm)	1.0	6.0	1.0	2.0	13.0	6.0	2.0	1.0	1.0	3.0
Ba (ppm)	18.0	79.0	239.0	214.0	204.0	315.0	259.0	236.0	248.0	-6.0
Sc (ppm)	1.3	#	1.1	3.5	#	42.0	1.3	3.4	1.1	#
Co (ppm)	8.0	8.0	97.0	23.0	11.0	25.0	7.0	67.0	75.0	67.0
V (ppm)	6.0	27.0	7.0	52.0	28.0	10.0	28.0	61.0	20.0	8.0
Ce (ppm)	7.0	17.0	6.0	13.0	17.0	1215.0	6.0	9.0	7.0	9.0
Nd (ppm)	5.0	#	0.0	3.0	0.0	670.0	0.0	2.0	1.0	#
La (ppm)	3.0	0.0	1.0	3.0	4.0	561.0	0.0	2.0	0.0	1.0
Cr (ppm)	6.0	#	3.0	12.0	#	2.0	12.0	11.0	5.0	#

Note: # Not analysed because of problems caused by high Ca and/or P. LOI – Lost On Ignition.

In contrast, the non-opalised ichthyosaur bone from Moon Plains, north of Coober Pedy, consists of bioapatite and high magnesium calcite, with only a small amount of silica. Trace element analyses of the sample, when normalized to the PAAS shale, also show that the bone is depleted in all trace elements with the exception of a slight enrichment of Sr. The elevated Sr level is probably a product of the carbonate-rich mineralogy.

The trace element patterns of these opalised samples of bone and wood from Australian fields can be contrasted with samples of opalised wood from Nevada. The Nevada opalised wood is enriched in U, (48.1 ppm compared to 0.2 ppm in White Cliff opalised wood), but like the opalised bone samples above, it is depleted in all trace elements compared to PAAS. The bulk composition of modern dolphin bone shows that it consists of bioapatite with water and organic material and trace element composition is broadly similar to the ichthyosaur bone from Moon Plain.

Phase Mineralogy

The X-ray diffraction traces for the bone samples are shown in Figure 1. The characteristic broad reflections for carbonatehydroxylapatite (bioapatite) are shown in the X-ray diffraction pattern of modern dolphin bone. These bioapatite reflections are also present in the diffraction pattern for the ichthyosaur limb bone from Moon Plain near Coober Pedy, but the reflections are somewhat sharper, indicating that the bioapatite crystals many have been recrystallised during diagenesis. This diffraction trace is dominated by the characteristic sharp reflections from magnesium calcite. This bone has been partially replaced by magnesium calcite. The magnesium calcite fills the central canals of the osteons and

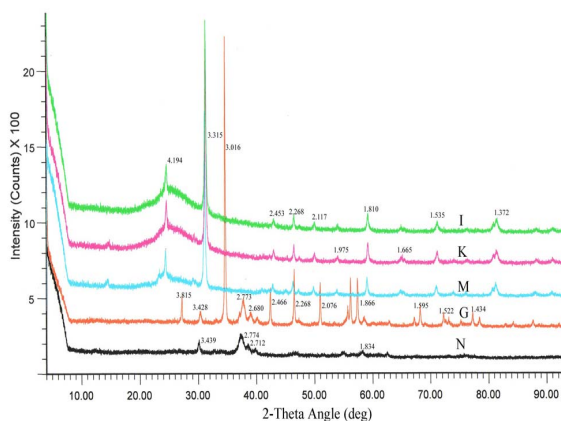


Figure 1: Stacked XRD traces of bone samples.

probably also impregnates the carbonatehydroxylapatite in the osteon microstructure (Figure 2).

The X-ray diffraction pattern for the three opalised plesiosaur bones are very similar and are dominated by the sharp reflections of quartz, with the three strongest lines being at 24.27° (4.255 \AA), 31.06° (3.343 \AA) and 59.58° (1.802 \AA). Note, however, the wide hump in the background between 22° and 30° 2θ , which is associated with the amorphous structure of opal A. This feature is somewhat less prominent in the plesiosaur limb/rib bone pattern (35618-A). There is no evidence of remnant bioapatite in these patterns, a finding consistent with the chemical analyses that show only trace amounts of Ca and no P. The bones have been completely replaced by opal and quartz with small amounts of clay minerals sometimes trapped in the osteon canals. The opal replaces the concentric fibrous structure of the osteons, with quartz in filling the canals (Figure 3).

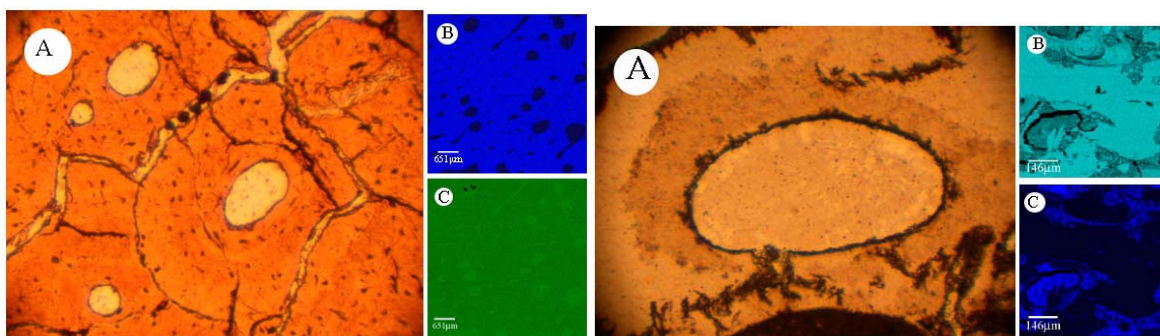


Figure 2 (left): A. Ichthyosaur plane light optical image; B. Phosphorus backscattered element map; C. Calcium backscattered element map.

Figure 3 (right): A. Opalised plesiosaur neural arch plane light optical image; B. Silicon backscattered element map; C. Aluminium backscattered element map.

The X-ray diffraction pattern of the opalised wood from Nevada shows strong reflections due to opal (CT) (tridymite opal), and its presence is consistent with the volcanic origins for this opalisation. The X-ray diffraction pattern for the opalised wood from White Cliffs corresponds to opal (A) and shows no evidence of reflections due to quartz (Figure 4).

The opalised wood from White Cliffs and the opalised plesiosaur bones from Andamooka are chemically very similar and reflect similar compositions for the opalising fluids. Differences in mineralogy, the presence of quartz in the opalised bone filling the osteon canals and the lack of quartz in the wood indicates that the process of opalisation may have been different between the two materials. The cell microstructure in the wood has not been preserved during opalisation: in this material it appears that precious opal has filled open cracks.

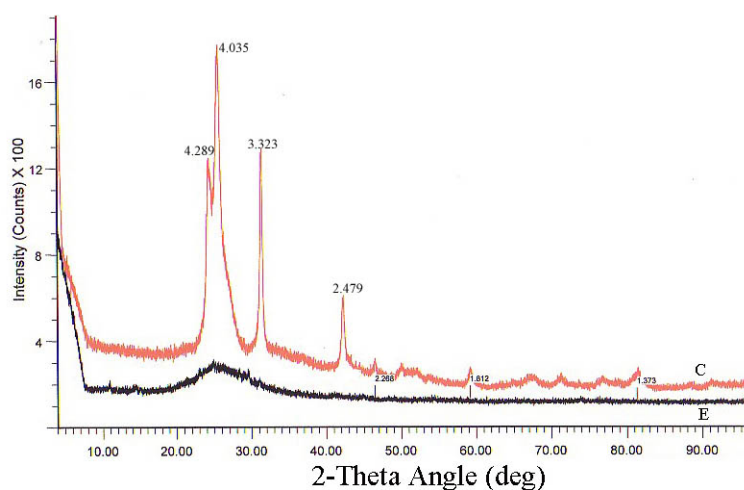


Figure 4: Stacked XRD traces of fossilized wood from Nevada (C) and opalised wood from White Cliffs (E).

DISCUSSION

The microstructure of the calcified ichthyosaur bone is shown in Figure 2a. The outlines of the osteons with their central canals, around $400 \mu\text{m}$ in diameter, are clear. The osteon canals are filled with magnesium calcite. The fine details of the concentric rings of bioapatite lamella and the black lacuna within the osteons are also preserved. This indicates that the crystallization of the bioapatite and the possible in-filling of gaps between the lamella occurred as tightly coupled reactions. The fluids moved through the canals that were later filled with magnesium calcite. Figure 3a shows the microstructure of one of the opalised plesiosaur bones. Again, the individual osteons and their central canals are clear, but much of the fine structure; concentric

rings of lamella and the lacuna, have not been preserved. The central canals are filled with fibrous quartz indicating that it may have crystallized from a gel filling the canals. The level of microstructural preservation in the opalised bone suggests that opalisation is not a closely coupled dissolution-reprecipitation reaction and that there was a fluid filled space between the reaction fronts. If we assume that the opalisation occurs before the canals are filled with quartz then the width of the gap between the dissolution front and the precipitation fronts must have been less than 100 μm . This distance is estimated on the level of microstructural detail that was preserved. This means that opal silica spheres, that are around 0.3 μm in diameter (Figure 5) must have formed and 'settled' within a comparatively small space. They did not form and then gently settle from solution as they do in synthetically grown opal (Darragh *et al.* 1977). Also the fact that the fine-scale features of the microstructure (concentric rings of lamella and the lacuna) were not preserved may indicate that the opal did not initially form as a gel and then solidify.

An alternative interpretation is that the fibrous quartz filled the osteon canals before opalisation and that the bioapatite was then dissolved away leaving a hollow cast that filled slowly with opal. The problem with this alternative interpretation is that if quartz filled the canals before opalisation, it would be reasonable to expect that the quartz would also have at least partially impregnated the fibrous bioapatite structure, but this has not been observed. We currently favour the former explanation over the latter, but more detailed studies are required before any firm conclusion can be drawn.

It is unclear at this stage whether the microstructural chemical and mineralogical observations reported here will shed any light on the timing of the opalisation event. The fact that the trace element analysis shows that these opalised fossils are depleted in uranium would seem to preclude the possibility radiometric dating opal formation.

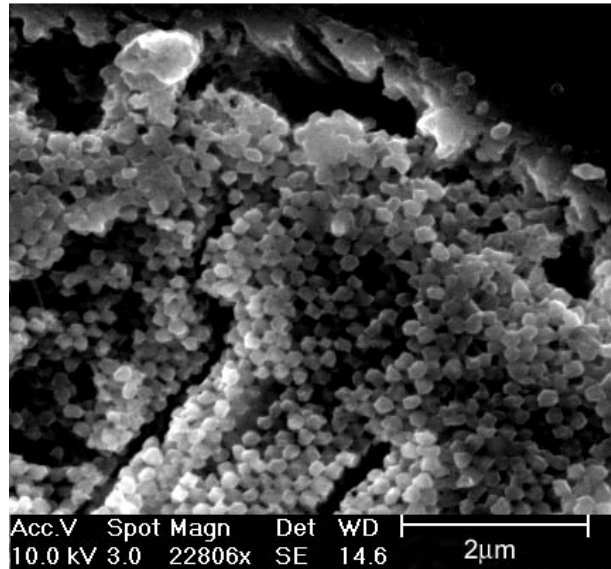


Figure 5: SEM image of an HF-etched polished block of opalised plesiosaur neural arch showing the gap between opal silica spheres and quartz.

REFERENCES

- BARKER I.C. 1980 *Geology of the Coober Pedy Opal Fields with special reference to the precious opal deposits*. University of Adelaide, unpublished M.Sc thesis.
- BARNES L.C., TOWNSEND I.J., ROBERTSON R.S. & SCOTT D.C. 1992. *Opal: South Australia's Gemstone*. South Australia Department of Mines and Energy.
- CORBETT G.J. & LEACH T.M. 1998. *Southwest Pacific rim gold-copper systems: structure, alteration and mineralization*. Society of Economic Geologists.
- DAY R.W. 1969. The Lower Cretaceous of the Great Artesian Basin. In: CAMPBELL K.S.W. ed. *Stratigraphy and Palaeontology: Essays in Honour of Dorothy Hill*. Australian National University Press, 140-173.
- DARRAGH P.J., GASKIN A.J. & SASNDERS J.V. 1977. Synthetic Opals. *Australian Gemmologist* **13**, 109-118.
- DOWELL K. & MAVROGENES J. 2004. Black Opal. *Geological Society of Australia Abstracts* **73**, p. 68.
- HORTON D. 2002. Australian Sedimentary Opal-Why is Australia Unique? *Australian Gemmologist* **21**, 287-294.
- HUBERT J.K., PANISH P.T., CHURE D.J. & PROSTAK K.S. 1996. Chemistry, microstructure, petrology and diagenetic model of Jurassic dinosaur bones, Dinosaur National Monument, Utah. *J. Sediment. Res.* **66**, 531-547.
- JONES J.B. & SEGNET E.R. 1966. The occurrence and formation of opal at Coober Pedy and Andamooka: *Australian Journal of Science* **29**, 129-133.
- KEAR B.P. 2003. Cretaceous marine reptiles of Australia: a review of taxonomy and distribution. *Cretaceous Research* **24**, 277-303.
- PUTNIS A. 2002. Mineral replacement reactions: from macroscopic observations to microscopic mechanisms. *Mineral. Mag.* **66**, 689-708.